# Fast Particle Losses in ITER

IT/P6-2

T. Kurki-Suonio[1], O. Asunta[1], V. Hynönen[1], T. Johnson[2], T. Koskela[1], J. Lönnroth[1], V. Parail[3], M. Roccella[4], G. Saibene[5], A. Salmi[1], and S. Sipilä[1]

[1] *Helsinki Univ. of Technology, Assn Euratom Tekes, PO Box 4100, 02015 TKK, Finland*
[2] *EURATOM-VR Assn, Fusion Plasma Physics, EES, KTH, 10044 Stockholm, Sweden*
[3] *EURATOM/UKAEA Fusion Assn, Culham Science Centre, Abingdon, OX14 3DB, UK*
[4] *L.T. Calcoli S.a.S., Piazza Prinetti 26/B, 23087 Merate (Lecco), Italy*
[5] *F4E, c/ Josep Pla n° 2, Torres Diagonal Litoral B3, 08019 Barcelona, Spain*

*The wall loads due to fusion alphas were simulated for ITER Reference Scenario-2 and Scenario-4 including the effects of ferritic inserts (FI) and Test Blanket Modules (TBM). The simulations were carried out using the Monte Carlo -based guiding center orbit-following code ASCOT. The ferritic inserts were found very effective in ameliorating the detrimental effects of the toroidal ripple: the fast ion wall loads are reduced practically to their axisymmetric level. The load is fairly evenly divided between the divertor and the limiter, with practically zero power flux to other components in the first wall. In contrast, uncompensated ripple leads to fairly high peak power fluxes of 0.5 MW/m$^2$ in Scenario-2 and 1 MW/m$^2$ in Scenario-4, with practically all power hitting the limiters and substantial flux arriving even at the unprotected first wall components. The local TBM structures were found to perturb the magnetic field structure globally and lead to increased the wall loads. However, the reliability of the TBM simulations suffers from over-simplifications in the vacuum field.*

## 1. Introduction

The new physics introduced by ITER operation, of which there is very little prior experience, is related to the very energetic (3.5 MeV) alpha particles produced in large quantities in fusion reactions. These particles not only constitute a massive energy source inside the plasma, but they also present a potential hazard to the material structures that provide the containment of the burning plasma.

The finite number (18 in ITER) and limited toroidal extent of the Toroidal Field (TF) coils cause a periodic variation of the toroidal field called the magnetic ripple. This ripple can provide a significant channel for fast particle losses, leading to localized fast particle loads on the walls. Because the ripple can cause significant additional ion transport, ferritic inserts (FIs), are being designed in the double wall structure of the ITER vacuum vessel in order to reduce the ripple. The toroidal field in ITER is further disturbed by the presence of the test blanket modules (TBM) used to test tritium breeding.

The ripple can increase the fast ion transport in three qualitatively different ways: 1) Local magnetic wells can form in between adjacent coils. An ion with sufficiently small parallel velocity can get trapped into one of these wells and will promptly escape the plasma practically vertically due to the gradient drift. These are called direct ripple losses. 2) Due to the toroidally varying field strength, subsequent banana turning points are vertically shifted. The orbits then no longer close in the poloidal plane. If the changes in turning point location get somehow uncorrelated, this leads to transport. When the decorrelation is caused by collisions, this is called ripple-banana diffusion. 3) When the ripple is very strong and/or the particle energy very high, the turning points can get intrinsically decorrelated leading to increased transport [1]. This is called stochastic ripple diffusion. In ITER magnetic geometry very little stochastic or direct ripple losses are expected. Indeed, the obtained wall loads do not exhibit any phase space structure that would support the presence of direct ripple losses.

We have simulated four fast ion species: alphas produced in thermonuclear reactions, NBI ions, ICRF-accelerated ions, and beam-target fusion alphas. Due to space limitations, only wall loads due to thermonuclear alphas that overwhelmingly dominate the loads will be presented. The wall loads were calculated in a variety of magnetic field configurations including two different designs of FIs and none or more TBMs. The simulations were performed using the 5D Monte Carlo guiding-center code ASCOT [2] that was significantly upgraded for this task. The wall loads were calculated for two ITER reference scenarios: Scenario-2 representing an inductive, standard H-mode operation of ITER, and Scenario-4 representing a steady-state operation [3]. No anomalous transport was accounted for.

## 2. ASCOT Simulations of Fusion Alphas in ITER

A new 3D magnetic field module was developed in order to interface ASCOT with the 3D vacuum field maps provided for the task. The magnetic data is assembled from separate 2D equilibrium and 3D vacuum fields. Also a 3-dimensional representation of the wall combined with finite Larmor radius effects was devised for the wall collision model.

Simulating high-energy particles is computationally very CPU-intensive due to the large velocity that requires a small time step and the low collisionailty that requires a very long simulation time before there are any significant changes in energy or orbit topology. Furthermore, the ITER simulations are exceptionally CPU-intensive due to the 3-dimensional interpolation needed for the realistic magnetic background. Therefore, *selective acceleration of interaction timescales* in which only strongly passing ions participate in the acceleration, has been used in the simulations.

The simulations were carried out for **seven** different magnetic backgrounds with $B_T =$ 5.3 T unless otherwise mentioned. An axisymmetric case (**no-ripple**) serves as a reference scenario when assessing ripple effects. The ripple-induced losses are then analyzed both in the presence and absence of ferritic inserts. The optimization of the distribution of ferrites depends on many factors, including the prospect of ITER operation at reduced toroidal field strength. Therefore two different configurations (**FI** and **opt-FI**) of inserts are considered and losses in the presence of FI are calculated also at half of the maximum field strength, $B_T = 2.65$ T (**opt-FI, 2.65 T**), to find out how the overcompensation of the ripple affects the fast ion losses. Finally, the worst scenarios including one or more TBM are studied (**opt-FI, 1 TBM** and **opt-FI, 2 TBM**).

The particles are simulated until they have slowed down to 100 keV, which can take several seconds per particle. Running ASCOT down to energy values corresponding to twice the local temperature did not noticeably alter the results. The quality of the simulations is diagnosed by the conservation of energy. Violation in energy conservation, predominantly due to the discreteness of the magnetic background data, for a particle slowing down from the MeV range to thermal energies of a few keV is typically only 1 – 2 % of its initial energy.

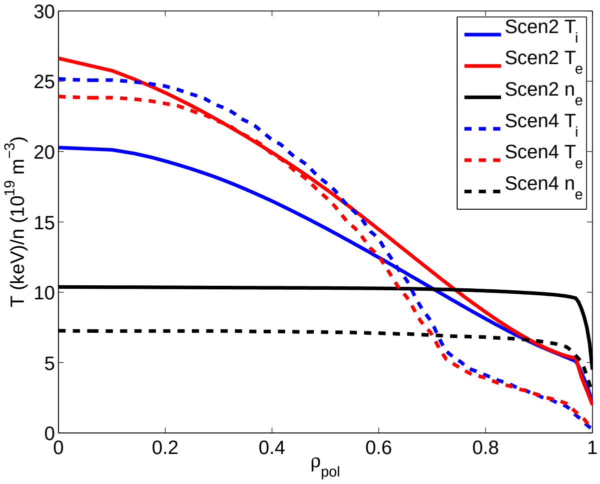


Figure 1: *Electron density and electron and ion temperature profiles in Scenarios 2 and 4. The concentrations of plasma species ($n_i/n_e$-%) were the following: D and T both 39.782 %, $^3$He 1.0 %, $^4$He 4.3 %, Be 2 % and Ar 0.102 %. This composition yields effective charge number of $Z_{eff}$ = 1.66.*

### 2.1. Scenario-2

The plasma profiles are illustrated in Fig. 1. The plasma current is 15 MA. The test particle weights were calculated from the fusion power density. The total fusion power, recalculated from the test particle weights, is 470 MW, and the power deposited onto alphas is 93.6 MW.

An overview of the simulated alpha wall loads in Scenario-2, together with the maximum ripple strength along the separatrix, is given in Table 1. A striking feature in Table 1 is the insensitivity of the divertor load to the ripple: it always stays at about its axisymmetirc level of 100 kW, while the limiter load varies by more than factor of five. This can be understood in terms of ripple diffusion that enhances the transport of trapped ions only. Since the limiter at the outer midplane is the material structure by far closest to the separatrix, the out-drifting trapped ion will intersect the limiter before it ever has a chance to approach the divertor. Introducing the TBMs, however, has a dramatic effect on the divertor loads. This is because, as will be discussed later, the local perturbation generated by the TBMs affects also the passing ions that can easily access the divertor. However, as will be shown, the TBM magnetic backgrounds used here overestimate this effect and, thus, the TBM results should be taken as tentative only.

**No ripple.** Figure 2 displays the distribution of the wall loads, and Figs. 3(a) and 4(a) show the probability distributions of final energies and initial $\rho$-surfaces of the lost ions, respectively. Almost all lost ions originate from very close to the separatrix and have energy close to their birth value, *i.e.*, they are most likely direct orbit losses. A small fraction of ions, still originating from near the separatrix, are lost at lower energies, due to collisions. The first orbit losses are distributed quite evenly between the limiter and the divertor, with a small number hitting the rest of the wall. The double-hump structure in the toroidally averaged distributions at the limiter location results from the fact that the limiter plate is not flat but, rather, has a knee at around the equatorial plane. Furthermore, the point closest to the wall along the separatrix is slightly above the horizontal midplane and, below the midplane, the shortest distance between the plasma and the wall is approximately at $\theta = -50°$.

**No-FI.** Figure 2 also shows the distribution of the wall loads when the maximum ripple strength along the separatrix reaches 1.1%. Compared to the axisymmetric case the most

Table 1: *Wall load from fusion alphas in Scenario-2 and Scenario-4.*

| Magnetic background | Max ripple % | Total wall load (kW) | Peak power flux (kW/m$^2$) | % of total alpha power | Limiter/ divertor (in kW) |
|---|---|---|---|---|---|
| no-ripple | 0 | 250 | 0.43 | 0.27 % | 130/115 |
| | 0 | 20 | 12 | 0.03 % | 10/5 |
| no-FI | 1.1 | 1040 | 500 | 1.10 % | 750/120 |
| | 1.1 | 2300 | 990 | 3.69 % | 2000/0 |
| FI | 0.32 | 420 | 440 | 0.45 % | 250/160 |
| opt-FI | 0.20 | 300 | 210 | 0.32 % | 180/110 |
| | 0.21 | 30 | 50 | 0.05 % | 25/0 |
| opt-FI 2.65 T | 0.7 | 40 | 22 | 0.69 % | 20/10 |
| | 0.71 | 100 | 70 | 2.55 % | 85/0 |
| opt-FI, 1 TBM | 1.1 | 650 | 380 | 0.70 % | 360/280 |
| | 1.1 | 75 | 100 | 0.16 % | 70/0 |
| opt-FI, 2 TBM | 1.1 | 780 | 530 | 0.83 % | 410/360 |
| | 1.1 | 75 | 100 | 0.17 % | 70/0 |

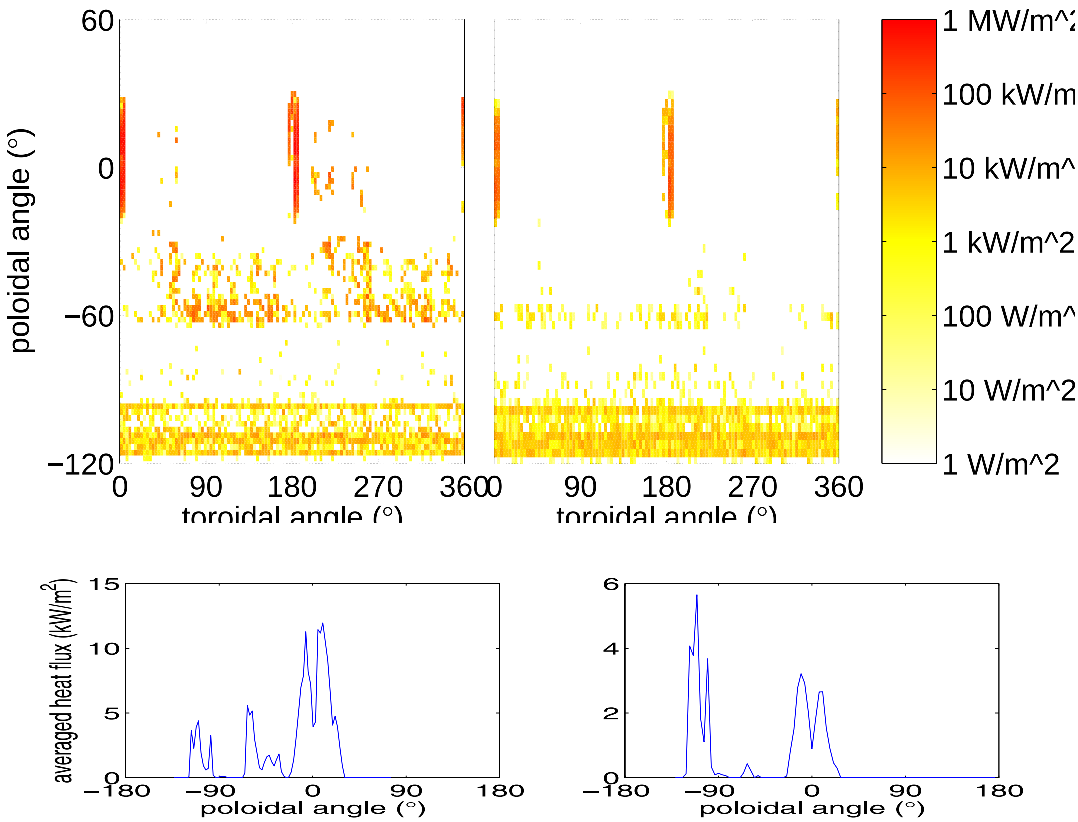


Figure 2: *(a) The 2D wall load distribution for uncompensated ripple (left) and axisymmetric field (right). (b) The corresponding toroidally averaged wall loads.*

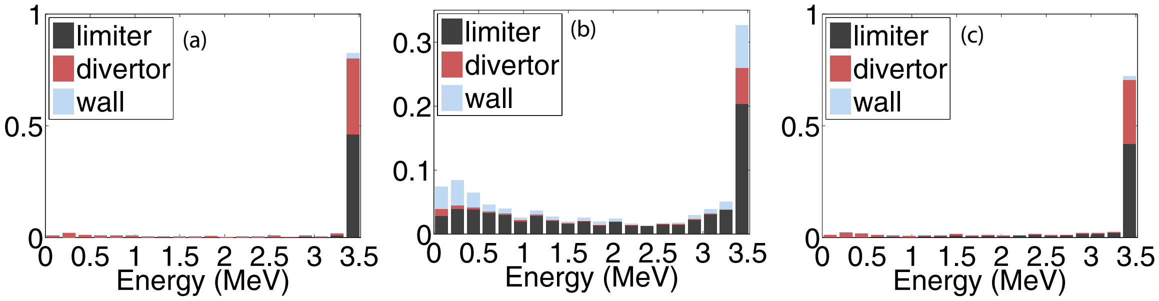


Figure 3: *The probability distribution of the final energy of thermal alphas lost to the wall in (a) axisymmetric case, (b) with uncompensated ripple, and (c) with optimized inserts.*

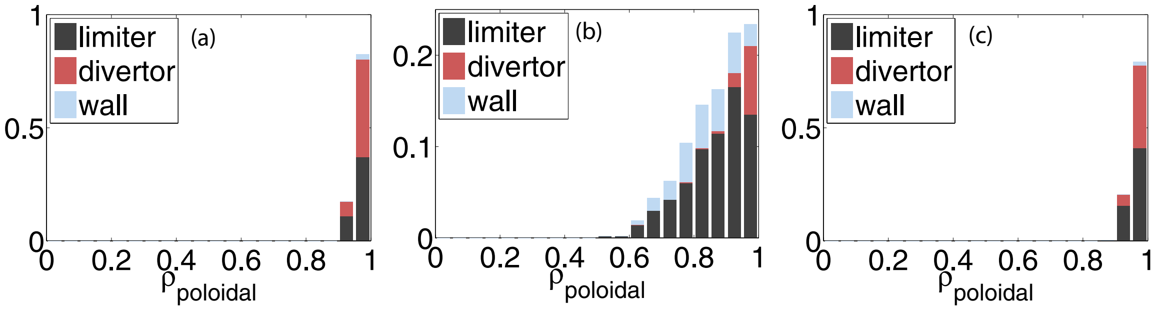


Figure 4: *The probability distribution of the birth location of thermal alphas in (a) axisymmetric case, (b) with uncompensated ripple, and (c) with optimized inserts.*

notable difference is in magnitude, but also the number of non-limiter, non-divertor hits has increased, forming a belt below the limiters that shows some structure corresponding to the gaps between the field coils. The energy distribution, Fig. 3(b), is now much more spread out, and a second peak is visible at low energies. Still, most particles are lost very close to their original energy. The initial position distribution, Fig. 4(b), shows that losses can now, due to the ripple-enhanced diffusion, originate from much deeper inside the plasma, down to $\rho = 0.6$.

**FI.** The maximum ripple strength along the separatrix is now reduced to 0.32%. The two notable differences to the no-FI case are the drop in total wall loads by over a factor of 2 and a slight increase in the divertor load. The limiter load drops almost to the axisymmetric level. The ferritic inserts thus efficiently confine the ripple-sensitive ions allowing them to slow down in the plasma before possibly ending up at the divertor.

**Opt-FI.** From Table 1 it is apparent that the optimized inserts reduce the wall load even further than the basic inserts. The distribution of the wall load is practically indistinguishable from that corresponding to the axisymmetric case. Also the probability distributions of the loss energy and the initial position, Figs. 3(c) and 4(c), show that, in terms of the wall loads and loss distributions, the optimized inserts come very close to the axisymmetric case. Unfortunately it was later discovered that the ITER wall might not have enough space for the ferritic inserts to be built according to the optimized configuration.

**Opt-FI, 2.65 T.** Also the plasma current, plasma density and temperature were cut in half to preserve the $q$-profile, Greenwald density and other critical parameters. The absolute magnitude of the wall load in the half-field case is small, as indicated by Table 1, but it should be kept in mind that the fusion source is now 1/16th of the original. The ratio of lost power to source power is larger by about a factor of two when compared to the full-field case. The increase is actually surprisingly small considering the multitude of ways the reduction of the field and profiles can affect the loads: the orbits are widened due to the lower plasma current, the thermalization time is prolonged, and the FI actually overcompensate the ripple. The limiters still remain the hot spots, but the load below the limiter is much more evenly distributed. The ions originate from much deeper in the plasma than with the full field and current.

**Opt-FI, 1 TBM.** The magnitude of the wall load is significantly increased from the case with the optimized inserts only, but the distribution on the limiter and the divertor remains the same. There is an increase in the portion of low-energy wall hits, which differs from the previous simulations. This would suggest that the TBM creates additional transport that drives the slowing-down particles out before they get fully thermalized. The average divertor load now exhibits high peaks. Low energy particles have small Larmor radii and, therefore, a much greater fraction of them makes it to the divertor. The TBM is located at $\phi = 20°$, but in the vicinity of this position no structures in the load distribution are found.

**Opt-FI, 2 TBM.** In ITER, the three TBMs will be adjacent to each other. However, in these simulations the second TBM was added 80° from the first to smoothly join the magnetic fields of adjacent sectors. A second TBM was nonetheless simulated in order to see whether it causes additional losses. However, very little difference to the 1 TBM case was found. This suggests that the first TBM shadows the second one, so that there are less particles left in the phase space affected by the second TBM.

### 2.2. Scenario-4

Scenario-4 has a plasma current of 9 MA, which is considerably lower than in Scenario-2 and is likely to result in poorer confinement of fast ions. Compared to Scenario-2, Scenario-4 has a much lower density and temperature at the edge of the pedestal, see Fig. 1. The total Scenario-4 fusion power is 310 MW, with 52 MW deposited onto alphas and its distribution is different: the fusion reactions are concentrated in the central region and the rate drops rapidly near the edge whereas in Scenario-2 the fusion density gradually decreases towards the edge.

According to Table 1 only with an uncompensated ripple can the alphas pose a threat to the walls. The total power load is 2.3 MW and the power load on the limiters reaches almost 1 $MW/m^2$ on the hot spots. The vast majority of the wall load is again on the limiters, and the divertor gets practically no power load. The belt of wall hits, found for Scenario-2, is visible here as well, though its correspondence to the ripple period is not as clear. The wall losses can now originate from anywhere in the plasma, a drastic change from the Scenario-2 simulations where the probability dropped to zero around $\rho = 0.6$. It thus appears that Scenario-4 with its lower current is much more vulnerable to ripple transport. Furthermore, due to low density and temperature in the region, the edge contribution is very small. The energy distribution is fairly uniform. The low energy hits originate from the center, while the high energy hits originate from closer to the edge.

The FIs have a much greater effect in Scenario-4. The total power load drops from the no-FI case by almost a factor of 100, whereas in Scenario-2 the factor was about 5. This

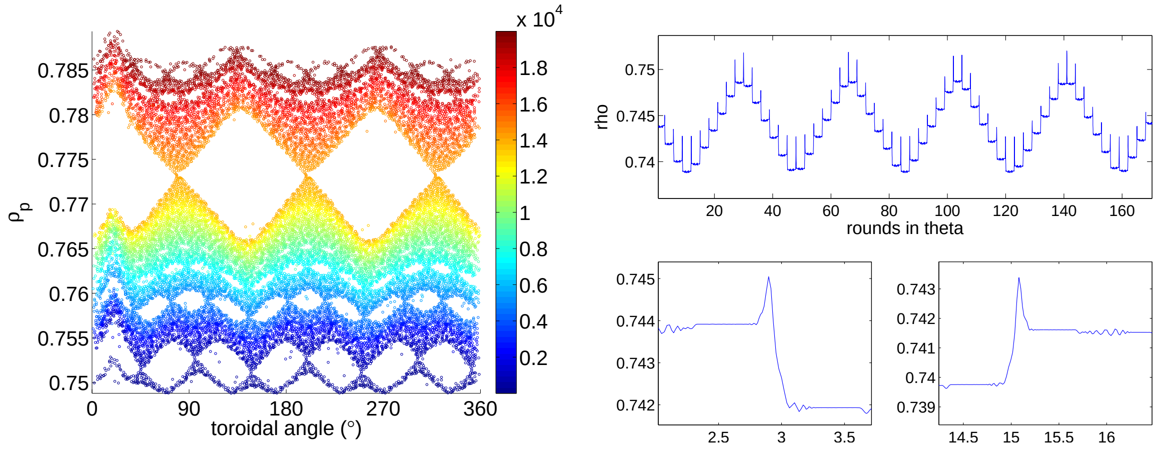


(a) (b)

Figure 5: *(a) A poincare plot of a 3.5MeV alpha particle's orbit as a function of the toroidal angle $\phi$ in the presence of a TBM at $\phi = 20\circ$. The particle has been followed for 20 000 poloidal orbits and the color tells the orbit number. (b) A field line in the vicinity of the 4,3 island, followed for 170 poloidal turns. The lower figures show blow-ups at the location of the radial kicks.*

confirms our interpretation of the high heat flux in the no-FI case being due to the ripple transport. Also the effect of reducing the field strength and current is larger in Scenario-4. The total power to the walls is then 2.5% of the source term, 50 times larger than in the full-field simulation. This increase is much larger than for Scenario-2 because, due to the large orbit widths, Scenario-4 is much more vulnerable also to the current reduction.

## 3. TBM Effects

ITER will have three TBMs, installed in horizontal ports, that are expected to disturb the magnetic field. The simulations soon revealed that a TBM does not cause toroidally localized particle losses but, rather, influences the wall load distribution globally. Figure 5(a) shows a Poincare plot of the orbit of a strongly passing ($\frac{v_\parallel}{v} = 0.9$) 3.5 MeV alpha particle, launched at $\rho = 0.7$, in the absence of collisions. A clear island structure emerges which, combined with the corresponding plot versus poloidal angle, reveals that the islands have distinct mode structure which, furthermore, is that of the local rational surface. The TBM, although local, modifies the edge magnetic field globally.

Figure 5(b) displays the flux surface coordinate of a fixed field line near the 4,3 rational surface as a function of poloidal revolutions. The effect of the coils is visible as small wiggles every time the field line traverses the low field side of the torus. An abrupt step in the radial location takes place only when the field line crosses the region in front of the TBM, which does not happen at every poloidal revolution. These radial kicks widen the rational surfaces into helical tubes, manifest in the figure as islands.

Such islands, if present in ITER, could also serve as seeds to a multitude of MHD modes. Fortunately the islands of present magnitude result at least partially from a simplification in the reconstruction of the 3D vacuum fields: The magnetic field adopted for the ASCOT simulations does not account for the ferritic response to the poloidal magnetic fields. This approximation may cause the islands to become too wide [1]. Islands could, however, appear even with a correct treatment of the ferritic response when accounting for the shear in the magnetic field between the TBM and the rational surfaces.

While the field lines are observed stationary along their orbits, the particles are found to drift slowly, in the matter of thousands of toroidal revolutions, due to these islands. As is clear from Fig. 5(a), this is the case even for strongly passing ions. This was also reflected in the wall loads reported for the TBM backgrounds. At this point it is still unclear if the drift is physical or not. The quantitative question of how large a physical drift the island structures can produce is currently investigated using Hamiltonian formalism.

## 4. Conclusions

In all simulated cases the fusion alpha load in ITER was found to be in the manageable level of about 1 $MW/m^2$ or less. The simulations show that the ferritic inserts, be they the basic or the optimized design, are very effective in ameliorating the detrimental effects of the toroidal ripple: the fast ion wall loads are reduced practically to their axisymmetric level. This is in good agreement with an earlier work carried out with the OFMC code using a 2-dimensional wall [4]. The load was found to be fairly evenly divided between the divertor and the limiter, with practically zero power flux to other components in the first wall. However, uncompensated ripple leads to the high peak power fluxes of 0.5 $MW/m^2$ in Scenario-2 and 1 $MW/m^2$ in Scenario-4, with practically all power hitting the limiters and noticeable flux arriving even at the unprotected first wall components. When reflecting on these optimistic results it should, however, be kept in mind that the effect of neither MHD activity nor micro-turbulence has been included.

This is the first time the effect of the TBMs has been studied. The TBMs were found to perturb the magnetic field structure globally and lead to enhanced fast ion transport and, thus, increased wall loads. The total wall load approaches that of the uncompensated ripple case, but its distribution on the wall is more benign with practically no power flux on the unprotected wall components. However, during the course of the work it was discovered that the magnetic backgrounds corresponding to the presence of the TBMs overestimate the perturbation.

This report was prepared as an account of work by or for the ITER Organization. The Members of the Organization are the People's Republic of China, the European Atomic Energy Community, the Republic of India, Japan, the Republic of Korea, the Russian Federation, and the United States of America. The views and opinions expressed herein do not necessarily reflect those of the Members or any agency thereof. Dissemination of the information in this paper is governed by the applicable terms of the ITER Joint Implementation Agreement. The computations presented in this document were made using the computing environment of the Finnish IT center for science, CSC. The work was partially supported by the Academy of Finland and EFDA/F4E.

**References**

[1] GOLDSTON, R.J. *et al.*, Phys. Rev. Lett. **47** (1981) 647.
[2] ITER Technical Basis 2001, http://www.iter.org/reports.htm
[3] HEIKKINEN, J.A. *et al.*, Phys. of Plasmas **2** (1995) 3724.
[4] TOBITA, K. *et al.*, Plasma Phys. Contr. Fusion **45** (2003) 133.

[1] Private communications with Prof. K. Lackner (IPP-Garching) with input from Dr Y. Kamada (JAEA).